Molecular Vision 2014; 20:488-496 <http://www.molvis.org/molvis/v20/488>
Received 8 October 2013 | Accepted 9 April 2014 | Published 11 April 2014

Adeno-associated virus type 8 vector–mediated expression of siRNA targeting vascular endothelial growth factor efficiently inhibits neovascularization in a murine choroidal neovascularization model

Tsutomu Igarashi,[1,2] Noriko Miyake,[2] Chiaki Fujimoto,[1] Chiemi Yaguchi,[1] Osamu Iijima,[2] Takashi Shimada,[2] Hiroshi Takahashi,[1] Koichi Miyake[2]

[1]Department of Ophthalmology, Nippon Medical School, Tokyo, Japan; [2]Department of Biochemistry and Molecular Biology, Division of Gene Therapy Research Center for Advanced Medical Technology, Nippon Medical School, Tokyo, Japan

Purpose: To assess the feasibility of a gene therapeutic approach to treating choroidal neovascularization (CNV), we generated an adeno-associated virus type 8 vector (AAV2/8) encoding an siRNA targeting vascular endothelial growth factor (VEGF), and determined the AAV2/8 vector's ability to inhibit angiogenesis.

Methods: We initially transfected 3T3 cells expressing VEGF with the AAV2/8 plasmid vector psiRNA-VEGF using the H1 promoter and found that VEGF expression was significantly diminished in the transfectants. We next injected 1 µl (3×10^{14} vg/ml) of AAV2/8 vector encoding siRNA targeting VEGF (AAV2/8/SmVEGF-2; n = 12) or control vector encoding green fluorescent protein (GFP) (AAV2/8/GFP; n = 14) into the subretinal space in C57BL/6 mice. One week later, CNV was induced by using a diode laser to make four separate choroidal burns around the optic nerve in each eye. After an additional 2 weeks, the eyes were removed for flat mount analysis of the CNV surface area.

Results: Subretinal delivery of AAV2/8/SmVEGF-2 significantly diminished CNV at the laser lesions, compared to AAV8/GFP (1597.3±2077.2 versus 5039.5±4055.9 μm^2; $p<0.05$). Using an enzyme-linked immunosorbent assay, we found that VEGF levels were reduced by approximately half in the AAV2/8/SmVEGF-2 treated eyes.

Conclusions: These results suggest that siRNA-VEGF can be expressed across the retina and that long-term suppression of CNV is possible through the use of stable AAV2/8-mediated siRNA-VEGF expression. In vivo gene therapy may thus be a feasible approach to the clinical management of CNV in conditions such as age-related macular degeneration.

Choroidal neovascularization (CNV) is a major complication that threatens the vision of patients with various retinal degenerative and inflammatory diseases, including pathologic myopia, ocular histoplasmosis [1,2], and, especially, age-related macular degeneration (AMD) [3,4], which is the most frequent cause of visual impairment in individuals over the age of 40 years in developed countries [5,6]. Vascular endothelial growth factor (VEGF) is a 45-kDa homodimeric glycoprotein that increases vascular permeability [7], stimulates angiogenesis [8], and is a specific endothelial cell mitogen [9]. VEGF also functions as a vasodilator and an anti-apoptotic, endothelial cell survival factor [10], expression of which is upregulated by hypoxia [11] and inflammatory mediators [12]. In addition, VEGF has pathogenic importance in cases of AMD, since VEGF contributes to the development of CNV in humans [13,14] and experimental CNV models [15]. The angiogenic actions of VEGF are mediated through its binding to two endothelium-specific receptor tyrosine kinases: Flt-1 (fms-like tyrosine kinase or VEGFR1) and Flk-1/KDR (fetal liver kinase or VEGFR2) [16,17], with the VEGF ligand showing at least 10-fold greater affinity for Flt-1 than Flk-1/KDR. We previously showed that neovascularization in a mouse CNV model is efficiently inhibited by type 8 adeno-associated viral (AAV) vectors mediating expression of flt-1 [18]. Clinically, moreover, inhibiting the VEGF pathway using a VEGF aptamer or an anti-VEGF antibody effectively suppresses the pathway's CNV-related activity [19-21].

The ability of siRNA to specially and potently down-regulate the expression of a target gene post-transcriptionally is based on the sequence-specific degradation of homologous target mRNA [22]. Intravitreous injections of siRNA have been shown to inhibit expression of selected genes, and specific siRNA targeting VEGF has been shown to prevent retinal or choroidal neovascularization in mice [23,24]. However, because of the short half-lives of these molecules in vivo, repeated intraocular injections of siRNA are frequently required for therapeutic benefit, which confers a high cumulative potential for local ocular complications. Gene transfer

Correspondence to: Koichi Miyake, Department of Biochemistry and Molecular Biology Nippon Medical School, 1-1-5 Sendagi, Bunkyo-ku, Tokyo 113-8602, Japan Phone: 81-3-3822-2131 (ext. 5240); FAX: 81-3-5814-8156; email: kmiyake@nms.ac.jp

mediated by a viral vector offers the possibility of targeted, sustained, and regulatable delivery of therapeutic levels of angiostatic proteins or small therapeutic molecules to the retina after only a single administration to the appropriate intraocular site. AAV vectors, in particular, have the ability to mediate efficient and stable transduction [25], and we have already shown that the AAV2/8 vector can be transduced into the retina [18]. Recently, Askou et al. showed siRNA targeting VEGF expression localized to RPE cells inhibited neovascularization in a murine CNV model using a self-complementary AAV type 8 vector (scAAV2/8) [26]. We have already reported that single-strand AAV2/8 (ssAAV2/8) mediated soluble Flt-1 (sFlt-1) inhibited neovascularization in a murine CNV model [18]. Our future final goal is combination gene therapy using shRNA strategy and sFlt-1. However, since the scAAV has a severe size limitation of the insert gene (within 2.4 kb), it is difficult to express anti-angiogenic agents such as sFlt-1 (4Kb) for combination therapy. Therefore, to analyze whether ssAAV2/8-mediated shRNA against VEGF is effective, in the present study, we assessed the effect of shRNA targeting VEGF using ssAAV2/8 when expressed in the photoreceptor and RPE cells in a murine CNV model.

METHODS

Plasmid construction: Three siRNA sequences targeting the mouse VEGF gene were selected (SmVEGF-1, SmVEGF-2, and SmVEGF-3; Figure 1) using siRNA design software (siDirect) [27]. To express shRNA, we chose the human H1 RNA polymerase III promoter, which was used in viral vector-mediated expression of shRNA and suppresses the target gene efficiently in vivo and in vitro [28,29]. After synthetic double-stranded oligonucleotides were introduced into the BglII and HindIII sites of the pSUPER vector (OligoEngine, Seattle, WA), the BamHI and KpnI fragment was cleaved and introduced into the corresponding restriction sites of pSP72. The EcoRI fragment was then cleaved from that plasmid and introduced into the corresponding restriction sites of the AAV vector plasmid (CAGS-Gal_B19-EGFP_SUB201) [30].

Treatment with siRNA plasmid in vitro: Since we used siRNA against murine VEGF but not human VEGF, to analyze the effect of siRNA, we chose mouse-derived 3T3 cells. 3T3 cells maintained in Dulbecco's modified Eagle's medium (DMEM; D-5546, Sigma-Aldrich, Louis, MO) supplemented with 8% fetal bovine serum (FBS) were seeded to a density of 1×10^5 cells/well in a 24-well plate and allowed to adhere overnight. The cells were then transfected using Lipofectamine 2000 (Life Technologies, Tokyo, Japan) diluted 1:25 in Opti-MEM (Life Technologies). Each siRNA-containing plasmid diluted (20 ng/µl) in Opti-MEM was first added to the transfection mix at a 1:1 ratio and incubated at room temperature for 5 min. Then after the plated cells were washed with Opti-MEM, the siRNA/transfection agent complexes (DNA (µg): Lipofectamine 2000 (µl) = 1:2) were added (500 ng/well), and the cells were incubated for 72 h in 8% FBS DMEM at 37 °C under 5% CO_2. Thereafter, the cells were trypsinized with 0.25% trypsin-EDTA (Sigma, St. Louis, MO) and centrifuged at 900 ×*g* for 5 min. The resultant cell pellets were washed in PBS (1X; 137 mM NaCl, 2.7 mM KCl, 8.1 mM Na_2HPO_4, 1.5 mM KH_2PO_4, 0.5 mM $MgCl_2$, pH 7.2; D-5773, Sigma-Aldrich) and centrifuged again at 900 ×*g* for 5 min at 4 °C. These cells were fixed using 1% paraformaldehyde (PFA)/PBS (Wako, Pure Chemical Industries, Tokyo, Japan) and analyzed with fluorescence-activated cell sorting (FACS; BD FACSCalibur, Becton, Dickinson and Company, Franklin Lake, NJ). These cells were also used to isolate total RNA.

Semiquantitative PCR for detection of VEGF expression: Total cellular RNA was extracted from each sample, treated with DNase 1, and purified using a RNeasy Mini Kit according to the manufacturer's instructions (Qiagen, Valencia, CA). cDNA was generated by reverse transcription of 150 ng of RNA using random hexamer primers and a TaKaRa RNA PCR Kit (AMV) Ver.3.0 (TaKaRa, Shiga, Japan). Real-time quantitative PCR was performed using Premix Ex Taq (TaKaRa) on a 7500 Fast Real-Time PCR System (Life Technologies) with the following primers and probes: for VEGF, 5′-GCA CTG GAC CCT GGC TTT ACT-3′ (forward), 5′-ACT TGA TCA CTT ATG GGA CTT CTG-3′ (reverse), and 5′-CCA TGC CCA GTG GTC CCA GGC TG-3′ (probe); for GAPDH, 5′-CAT CAC TGC CAC CCA GAA GA-3′ (forward), 5′-ATG TTC TGG GCA GCC-3′ (reverse), and 5′-TGG ATG GCC CCT CTG GAA AGC TG-3′ (probe). The cycling protocol entailed incubation at 95 °C for 30 s followed by 40 cycles of 95 °C for 5 s and 60 °C for 34 s. Relative gene expression was calculated using the standard

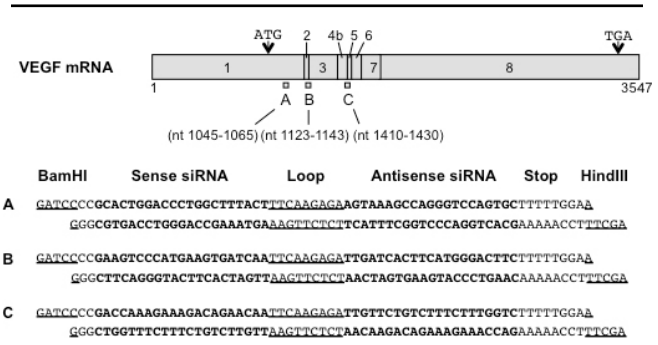

Figure 1. Schematic diagram showing the binding locations within human VEGF mRNA of the three siRNAs tested and the siRNA sequences. Sense and antisense siRNA sequences are shown in bold, and loop sequences and restriction sites (BamHI and HindIII) are underlined.

curve method. The VEGF mRNA levels were normalized to those of the housekeeping gene GAPDH. Each sample was run in duplicate, and each real-time PCR was repeated three times.

Generation of AAV vectors: An AAV2/8 vector encoding siRNA targeting VEGF (AAV2/8/SmVEGF-2) and a control vector encoding GFP (AAV2/8/GFP) were generated using an adenovirus-free system and purified using a previously described discontinuous iodixanol gradient centrifugation method [31]. In brief, the viral solution was layered with Optiprep (iodixanol; Axis-Shield plc, Oslo, Norway). Then after iodixanol continuous gradient centrifugation at 100,000 ×g for 15 h at 16 °C, the viral fractions were collected from the bottom of the gradient. The purified virion titers were determined with quantitative PCR analysis (Igarashi et al., 2013) [31]. The AAV2/8/GFP and AAV2/8/SmVEGF-2 titers were 3×10^{14} vector genomes (vg)/ml.

Animals: For the ocular injections, C57BL/6J mice were purchased from Charles River Laboratories Japan (Tokyo, Japan) and maintained under a 12 h:12 h light-dark cycle. All protocols involving animals were conducted in accordance with the Animal Experimental Ethical Review Committee of Nippon Medical School and the Association for Research in Vision and Ophthalmology (ARVO) Statement on the Use of Animals in Ophthalmic and Vision Research.

Histology: To confirm the location of gene transduction following subretinal injection of the vectors, 2-month-old mice were anesthetized, and 1 µl of AAV2/8/GFP was administered. Two months later, the eyes were enucleated, fixed overnight in 4% PFA/PBS at 4 °C, and sequentially transferred every 3 h to PBS containing 10%, 20%, or 30% sucrose. The eyes were then frozen in optimal cutting temperature (OCT) compound on dry ice, after which 6-µm cryostat sections were cut in a plane parallel to the vertical meridian of the eye. The sections were mounted using a medium containing 4, 6-diamidino-2-phenylindole (DAPI; Vector Laboratories, Burlingame, CA) and observed under a fluorescence microscope (Olympus, Tokyo, Japan). In addition, to assess the extent of the transfected surface following subretinal injection of the vectors, retinal flat mounts were made 2 weeks after injection, as described previously [31].

Generation of a murine laser photocoagulation-induced choroidal neovascularization model: To generate the CNV model, 2-month-old male C57BL/6 mice were first deeply anesthetized by intramuscular injection of ketamine hydrochloride (50 mg/kg; Daiichi Sankyo Company, Tokyo, Japan) and intraperitoneal injection of pentobarbital sodium (50 mg/kg; Kyoritsu Seiyaku Corp, Tokyo, Japan). The experimental CNV model was then created as preciously described [18]. Briefly, the beam from a diode laser (532 nm; Lumenis, Yokneam, Israel) was shone onto to the retina through a slit-lamp biomicroscope using a 22-mm cover glass as a contact lens. The treatment parameters were chosen to produce a cavitation bubble in the choroid without hemorrhage (spot size, 100 μm^2; intensity, 120 mW; duration, 100 ms). Four laser burns were made at the 3, 6, 9, and 12 o'clock positions of the posterior pole, around the optic nerve in both eyes. One week before the laser treatment, 1 µl of AAV2/8/GFP or AAV2/8/ SmVEGF-2, was delivered by subretinal injection at the posterior limbus using a Hamilton syringe (Hamilton Inc., Reno, NV) with a 33-gauge needle.

Detection of choroidal neovascularization using fluorescein angiography: Two weeks after the laser treatment, the size of the CNV lesions was measured in the choroidal flat mounts [18]. Anesthetized mice were killed by cardiac perfusion of 40 ml of PBS, 5 ml of PFA/PBS in PBS, and 2 ml of a mixture of fluorescein-isothiocyanate (FITC)-conjugated high-molecular-weight dextran (molecular weights: 2×10^6 and 4×10^4 Da in a proportion of 2:1 at a concentration of 10 mg/ml; Sigma). The eyes were then enucleated and fixed in 4% PFA/PBS overnight at 4 °C. A technique for visualizing FITC-dextran-perfused vessels within CNV was modified to enable simultaneous visualization of cell nuclei within the lesions. The anterior segment and the neurosensory retina were removed, and four radial relaxing incisions were made in the remaining sclera-choroid-RPE complex. Green FITC fluorescence from within the neovascular complexes was then visualized using a fluorescence microscope (Olympus DP50, Olympus), and the images were taken using a cooled charge-coupled device (CCD) camera. Although the retina of the control group (AAV2/8/GFP) expressed GFP that was detected at a wavelength similar to FITC-dextran, it was not difficult to distinguish RPE cells and vascular complex due to their morphology. The margins of the CNV lesion were defined with the FITC-dextran fluorescence and determined using image-analysis software (Photoshop CS5 extended; Adobe, Tokyo, Japan). The lesion sizes of AAV2/8/SmVEGF-2 (n = 12) and AAV2/8/GFP (n = 14) were averaged for each group. Data are presented with the means ± standard deviation (SD).

VEGF enzyme-linked immunosorbent assay: Two weeks after laser photocoagulation, the sclera-choroid-RPE complex and the neurosensory retina were isolated from AAV2/8/GFP and AAV2/8/SmVEGF-2 (each; n = 16). Thereafter, two samples from the sclera-choroid-RPE complex and the neurosensory retina were placed in 200 µl of 0.9% NaCl and homogenized, and the sclera was removed from the RPE/choroid complex. The resultant lysate was centrifuged at 17,000 ×g for 5 min

at 4 °C, and the VEGF levels in 50-µl aliquots of supernatant were determined using a Mouse VEGF Quantikine ELISA kit according to the manufacturer's protocol (R&D system, Minneapolis, MN).

Statistical analysis: Morphometric data from the different lesions in each eye were averaged to provide one value per eye. The mean and standard deviation (SD) for these measures for each group were calculated, and the Student *t* test was used to compare the groups (Microsoft Excel, Microsoft, Redmond, WA). In all cases, values of $p<0.05$ were considered statistically significant.

RESULTS

Suppression of VEGF expression in 3T3 cells: The 3T3 cells transfected with each of three AAV vector plasmids encoding siRNA targeting VEGF were examined using semi-quantitative real-time PCR. The transfection efficiency was nearly 65% (Figure 2A; pGFP; 65.22±15.65, pSmVEGF-1; 65.62±5.38, pSmVEGF-2; 67.29±11.42, pSmVEGF-3; 69.03±9.44), and VEGF expression was reduced by up to 55% in the cells treated with AAV2/8/SmVEGF (Figure 2B; pSmVEGF-1; 0.76±0.14, pSmVEGF-2; 0.55±0.14, pSmVEGF-3; 0.55±0.08). Somewhat stronger VEGF suppression was achieved with pSmVEGF-2 and pSmVEGF-3 than pSmVEGF-1 (*p*SmVEGF-1, *p*SmVEGF-2, *p*SmVEGF-3:0.77, 0.55, 0.55), so we selected pSmVEGF-2 for use in the subsequent in vivo experiments.

Widespread transduction by AAV8/GFP vector: To deliver the siRNA into the RPE cells responsible for VEGF expression, we chose a type 8 AAV vector, which we previously showed mediated highly efficient transduction [18]. Then to confirm which areas of the retina were transduced following subretinal injection of the AAV2/8/GFP vector, we performed a histological analysis of GFP expression using frozen sections and flat mounts. In frozen sections, GFP fluorescence was detected in photoreceptors and RPE cells from all injected eyes (n = 3; Figure 3A,B). Similarly, widespread GFP fluorescence was observed in RPE cells in the retinal flat mounts (n=3; Figure 3C,D).

Decrease in choroidal neovascularization lesions: We next investigated the efficacy of AAV2/8/ SmVEGF-2 in a murine laser photocoagulation-induced CNV model. The ability to inhibit angiogenesis was analyzed using the choroidal flat mount method [18]. In the case of the AAV2/8/GFP group, the RPE cells expressed GFP. However, it is not difficult to distinguish between GFP and CNV, as shown in Figure 4A–C. We found that CNV was significantly inhibited in the mice treated with AAV2/8/ SmVEGF-2 (n = 12), compared with the mice treated with AAV2/8/GFP (Figure 4F; 1597.3±2077.2 versus 5039.5±4055.9 µm^2; n = 14, $p<0.014$). Thus, subretinal injection of AAV2/8/ SmVEGF-2 was an effective treatment for CNV in our murine model.

Suppression of VEGF in RPE cells: Finally, we analyzed the VEGF level in the RPE/choroid complex and the neurosensory retina using a specific ELISA in treated mice. We found that the VEGF levels were slightly reduced in the neurosensory retina of the AAV2/8/SmVEGF-2 treated mice compared to the control AAV2/8/GFP mice (3.41 versus 3.84 pg/eye;

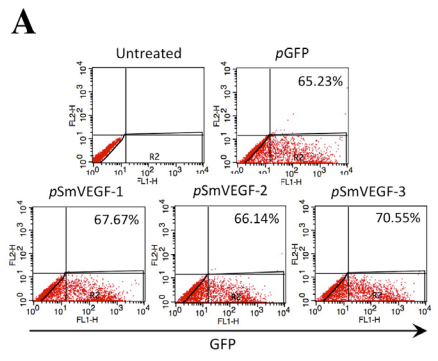

Transfection efficiency / GFP positive cells (%)

Vector	Exp 1	Exp 2	Exp 3	(Mean ± SD)
*p*GFP	49.57	80.87	65.23	65.22 ± 15.65
*p*SmVEGF-1	69.67	67.67	59.51	65.62 ± 5.38
*p*SmVEGF-2	56.49	79.24	66.14	67.29 ± 11.42
*p*SmVEGF-3	58.93	77.62	70.55	69.03 ± 9.44

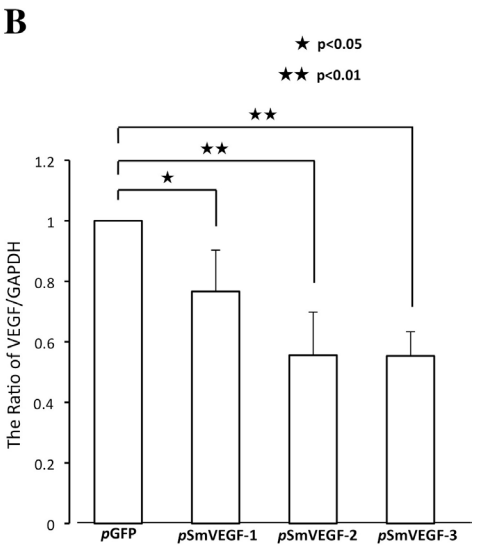

Figure 2. Transfection efficiency and siRNA-mediated vascular endothelial growth factor (VEGF) knockdown in 3T3 cells. **A**: Green fluorescent protein (GFP)-positive cells were measured using fluorescence –activated cell sorting (FACS) analysis. The transfection efficiency was nearly 65%. **B**: Efficacy screening of three siRNAs in 3T3 cells using semiquantitative RT–PCR. Note that the VEGF/GAPDH ratio was significantly smaller in cells transfected with the indicated SmVEGFs than the control vector. (*p*SmVEGF-1, *p*SmVEGF-2, *p*SmVEGF-3:0.77, 0.55, 0.55).

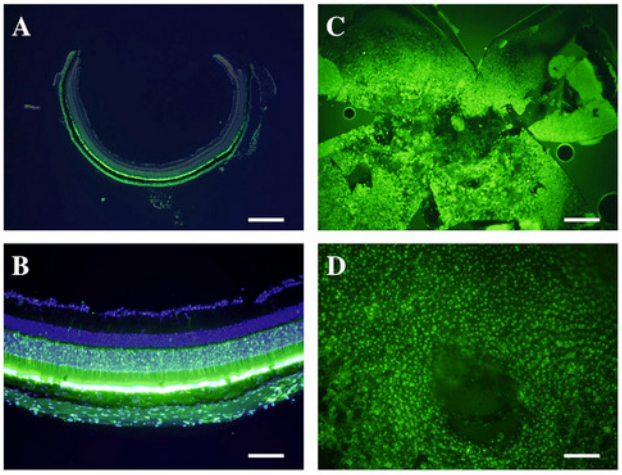

Figure 3. Histological analysis of green fluorescent protein expression. Expression mediated by the adeno-associated virus type 8 vector/green fluorescent protein (AAV2/8/GFP) vector was strongly detected in the photoreceptor cells and RPE cells after subretinal injection (**A** and **B**). Retinal flat mount preparations also showed widespread GFP expression in RPE cells (**C** and **D**). Scale bar = 500 µm; **A** and **C**, 100 µm; **B** and **D**.

Figure 5B). However, significant suppression of the VEGF level was observed in the RPE/choroid complex from mice treated with AAV2/8/SmVEGF-2 compared with AAV2/8/GFP (3.6 versus 6.06 pg/eye, p=0.0182) (Figure 5A). Thus, exogenous expression of siVEGF suppressed VEGF in this murine CNV model.

DISCUSSION

Among the various strategies proposed to prevent choroidal neovascularization in mice, administering siRNA specifically targeting VEGF [23] or VEGF receptor 1 [24] has proved effective. However, groundbreaking clinical trials of naked VEGF-A siRNA (bevasiranib) and VEGF receptor 1 siRNA (siRNA-027) [32,33] were suddenly halted due to adverse side effects, and the primary endpoints were never reached. Kaiser et al. reported some efficacy with lower doses, but not with the higher range of doses [33]. It was also reported that although siRNAs composed of 21 nucleotides (nt) or more suppressed CNV, the effect was unrelated to an RNAi action; instead, the siRNA activated cell surface toll-like receptor-3 (TLR3) in a sequence- and target-independent manner [34]. Consistent with that finding, two independent groups similarly reported that non-targeted 21-nt siRNA suppressed CNV [35,36]. In addition, Kleinman et al. demonstrated that non-internalized siRNAs induce retinal degeneration in mice by activating surface TLR3 on RPE cells [37]. They

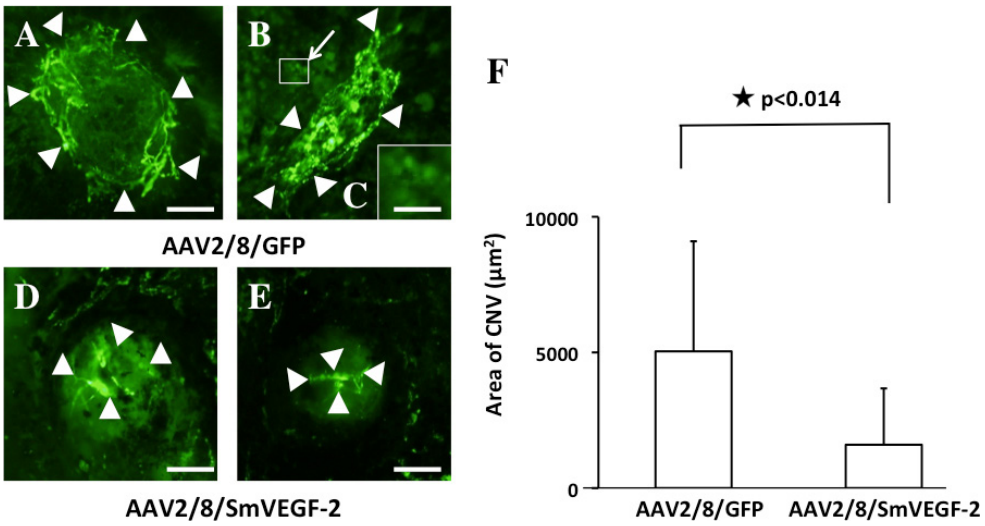

Figure 4. Efficient suppression of choroidal neovascularization in vivo. One week after subretinal injection of adeno-associated virus type 8 vector/vascular endothelial growth factor (VEGF) AAV2/8/SmVEGF-2 (n = 12) or AAV2/8/GFP (n = 14), mice were subjected to laser injury. After an additional 2 weeks the eyes were examined, and choroidal neovascularization (CNV) was analyzed using fluorescein angiography. CNV lesions in eyes injected with AAV2/8/SmVEGF-2 (**D** and **E**) were smaller than those in eyes injected with AAV2/8/green fluorescent protein (GFP; **A** and **B**). **C**: The magnification of square in the (**B**) showed the expression in RPE cells. Arrowheads: CNV lesions. Scale bar = 50 µm. **A**, **B**, **D**, and **E**, 150 µm; **C**.

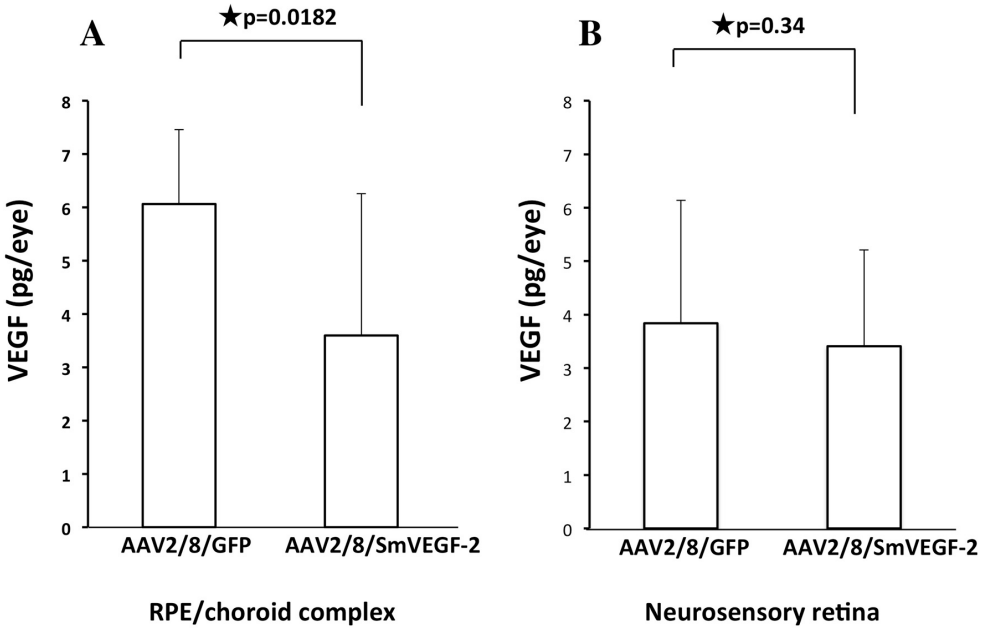

Figure 5. VEGF levels in RPE/choroid complex. Using a specific enzyme-linked immunosorbent assay (ELISA), VEGF levels were measured in cells transduced using adeno-associated virus type 8 vector/green fluorescent protein (AAV2/8/GFP) or AAV2/8/SmVEGF-2. AAV2/8/SmVEGF-2 suppressed VEGF expression in a murine choroidal neovascularization (CNV) model.

also suggested that evasion of immune system recognition might be accomplished through the use of siRNA duplexes shorter than 21 nt.

These observations suggest injection of naked siRNA may cause side effects by acting via TLR3 in the cytoplasm. However, this may be avoided by generating siRNA through virally mediated gene expression, as this siRNA could directly interact with targeted nucleic acid sequences in the nucleus. TLR3-dependent suppression on angiogenesis has also been seen in the laser-induced CNV model [33,37]. Consistent with the hypothesis of a TLR3 pathway proposed by Kleinman et al. [37], it may be that siRNA administration can trigger nonspecific autoimmune diseases, including uveitis, as siRNA may activate TLR3 on the cell surface and mimic a viral infection. Furthermore, repetitive activation of TLR3 by external siRNA may induce immune tolerance, which could also have adverse effects. We therefore strongly suggest that, for clinical application (e.g., for AMD), the delivery of siRNA encoded by an AAV vector is superior to repetitive external administrations of siRNA, and that viral delivery of siRNA gene is a potentially variable approach to treatment.

We confirmed that GFP is efficiently expressed following subretinal injection of AAV2/8/GFP in mice, and that the GFP expression was localized to photoreceptor cells and RPE cells. Some groups have reported that exogenous gene expression is limited to the bleb area following subretinal injection [38,39], while others reported that the area of expression extended over the entire retina [40,41]. We recently reported that the average relative area of GFP expression (the expression area/the whole area) following subretinal injection of AAV type 8 GFP was 18.0±18.9% in the neural retina and 29.3±25.8% in the RPE cells [31]. We suggested that the transduction efficiency depends on various factors, including the injection site, vector volume, viscosity, titer, and the age of injected mice. In the experiment of Askou et al., GFP expression was limited in the RPE cells [26]. They commented that effective titers below a particular threshold could lead to inefficient photoreceptor transduction. Our earlier findings indicate that AAV2/8/GFP can be used for photoreceptor transduction [18,31]. Askou et al. reported that AAV-mediated gene transfer of siRNA targeting VEGF did not reduce the diameter of CNV, but decreased the horizontal extension of CNV measured in retinal cross-sections. In contrast, we observed that AAV-mediated siRNA decreased the CNV size in retinal flat mounts. Moreover, we examined whether AAV2/8/SmVEGF-2 decreased VEGF expression using the ELISA system in the RPE/sclera complex and the neurosensory retina. VEGF levels were significantly decreased in the RPE/choroid complex, but were not decreased in the neurosensory retina. We suggested that the decrease in VEGF in the RPE/choroid complex led to the downsizing of CNV, since the VEGF level in the RPE/sclera complex was higher than in the neurosensory retina.

We previously investigated the inhibition of ocular neovascularization through lentivirus-mediated expression of angiostatin [42] and AAV2/8-mediated expression of soluble flt-1 [18]. Flt-1 is a member of the VEGF receptor family,

and we showed that soluble flt-1 inhibited CNV by blocking the activity of VEGF. This is noteworthy since siRNA suppresses the production of VEGF, but it does not affect VEGF already present. Lawrence et al. therefore suggested using a combination of siRNA-VEGF and ranibizumab [32]. Similarly, we suggest AAV-mediated expression of siRNA-VEGF and soluble flt-1 may be an effective approach to anti-angiogenesis therapy. In the case of sufficient and rapid expression of shRNAs, self-complementary (sc) AAVs might be preferable. However, since scAAV have a severe size limitation of the insert gene (within 2.4 kb), it is difficult to express anti-angiogenic agents such as Flt-1. In the present study, we assessed the effect of siRNA targeting VEGF using single-strand AAV type 8 vector (ssAAV2/8) when expressed photoreceptor and RPE cells in a murine CNV model. To develop the combination therapy, in this experiment, we used the single strand AAV vector used in a previous report [18], and suppression of CNV is possible through the use of stable ssAAV2/8-mediated siRNA-VEGF expression. These results indicated that ssAAV2/8/SmVEGF-2 is useful for combination therapy.

In summary, we have shown that type 8 ssAAV-mediated siRNA-VEGF expression decreased VEGF and inhibited CNV in an experimental model of CNV. This finding demonstrates the feasibility of an in vivo gene therapeutic approach to the clinical management of CNV in conditions such as AMD.

ACKNOWLEDGMENTS

This work was supported in part by Grant-in-Aid for Young Scientists (B) (23792014) from the Ministry of MEXT (Ministry of Education, Culture, Sports, Science and Technology, Japan) and Grant (S0801034) from MEXT-supported program for the strategic research foundation at private universities, 2008-2012. We thank Dr. James Wilson at the University of Pennsylvania for providing AAV packaging plasmids (*pac*H and p5E18-VD2/8). We also thank Yukihiko Hirai for making AAV viral vectors and Nagisa Asakawa and Maika Kobayashi for technical assistance.

REFERENCES

1. Hotchkiss ML, Fine SL. Pathologic myopia and choroidal neovascularization. Am J Ophthalmol 1981; 91:177-83. [PMID: 6162388].
2. Sickenberg M, Schmidt-Erfurth U, Miller JW, Pournaras CJ, Zografos L, Piguet B, Donati G, Laqua H, Barbazetto I, Gragoudas ES, Lane AM, Birngruber R, van den Bergh H, Strong HA, Manjuris U, Gray T, Fsadni M, Bressler NM. A preliminary study of photodynamic therapy using verteporfin for choroidal neovascularization in pathologic myopia, ocular histoplasmosis syndrome, angioid streaks, and idiopathic causes. Arch Ophthalmol 2000; 118:327-36. [PMID: 10721954].
3. Young RW. Pathophysiology of age-related macular degeneration. Surv Ophthalmol 1987; 31:291-306. [PMID: 3299827].
4. Starr CE, Guyer DR, Yannuzzi LA. Age-related macular degeneration. Can we stem this worldwide public health crisis? Postgrad Med 1998; 103:153-6. [PMID: 9590992].
5. Congdon N, O'Colmain B, Klaver CC, Klein R, Munoz B, Friedman DS, Kempen J, Taylor HR, Mitchell P. Causes and prevalence of visual impairment among adults in the United States. Arch Ophthalmol 2004; 122:477-85. [PMID: 15078664].
6. Coleman HR, Chan CC, Ferris FL 3rd, Chew EY. Age-related macular degeneration. Lancet 2008; 372:1835-45. [PMID: 19027484].
7. Senger DR, Galli SJ, Dvorak AM, Perruzzi CA, Harvey VS, Dvorak HF. Tumor cells secrete a vascular permeability factor that promotes accumulation of ascites fluid. Science 1983; 219:983-5. [PMID: 6823562].
8. Keck PJ, Hauser SD, Krivi G, Sanzo K, Warren T, Feder J, Connolly DT. Vascular permeability factor, an endothelial cell mitogen related to PDGF. Science 1989; 246:1309-12. [PMID: 2479987].
9. Ferrara N, Houck KA, Jakeman LB, Winer J, Leung DW. The vascular endothelial growth factor family of polypeptides. J Cell Biochem 1991; 47:211-8. [PMID: 1791185].
10. Alon T, Hemo I, Itin A, Pe'er J, Stone J, Keshet E. Vascular endothelial growth factor acts as a survival factor for newly formed retinal vessels and has implications for retinopathy of prematurity. Nat Med 1995; 1:1024-8. [PMID: 7489357].
11. Shweiki D, Itin A, Soffer D, Keshet E. Vascular endothelial growth factor induced by hypoxia may mediate hypoxia-initiated angiogenesis. Nature 1992; 359:843-5. [PMID: 1279431].
12. Cheng T, Cao W, Wen R, Steinberg RH, LaVail MM. Prostaglandin E2 induces vascular endothelial growth factor and basic fibroblast growth factor mRNA expression in cultured rat Muller cells. Invest Ophthalmol Vis Sci 1998; 39:581-91. [PMID: 9501870].
13. Kvanta A, Algvere PV, Berglin L, Seregard S. Subfoveal fibrovascular membranes in age-related macular degeneration express vascular endothelial growth factor. Invest Ophthalmol Vis Sci 1996; 37:1929-34. [PMID: 8759365].
14. Hera R, Keramidas M, Peoc'h M, Mouillon M, Romanet JP, Feige JJ. Expression of VEGF and angiopoietins in subfoveal membranes from patients with age-related macular degeneration. Am J Ophthalmol 2005; 139:589-96. [PMID: 15808152].
15. Yi X, Ogata N, Komada M, Yamamoto C, Takahashi K, Omori K, Uyama M. Vascular endothelial growth factor expression in choroidal neovascularization in rats. Graefes Arch Clin Exp Ophthalmol 1997; 235:313-9. [PMID: 9176680].

16. de Vries C, Escobedo JA, Ueno H, Houck K, Ferrara N, Williams LT. The fms-like tyrosine kinase, a receptor for vascular endothelial growth factor. Science 1992; 255:989-91. [PMID: 1312256].

17. Mustonen T, Alitalo K. Endothelial receptor tyrosine kinases involved in angiogenesis. J Cell Biol 1995; 129:895-8. [PMID: 7538139].

18. Igarashi T, Miyake K, Masuda I, Takahashi H, Shimada T. Adeno-associated vector (type 8)-mediated expression of soluble Flt-1 efficiently inhibits neovascularization in a murine choroidal neovascularization model. Hum Gene Ther 2010; 21:631-7. [PMID: 20053138].

19. Gragoudas ES, Adamis AP, Cunningham ET Jr, Feinsod M, Guyer DR. Pegaptanib for neovascular age-related macular degeneration. N Engl J Med 2004; 351:2805-16. [PMID: 15625332].

20. Ng EW, Shima DT, Calias P, Cunningham ET Jr, Guyer DR, Adamis AP. Pegaptanib, a targeted anti-VEGF aptamer for ocular vascular disease. Nat Rev Drug Discov 2006; 5:123-32. [PMID: 16518379].

21. Rosenfeld PJ, Brown DM, Heier JS, Boyer DS, Kaiser PK, Chung CY, Kim RY. Ranibizumab for neovascular age-related macular degeneration. N Engl J Med 2006; 355:1419-31. [PMID: 17021318].

22. Elbashir SM, Harborth J, Lendeckel W, Yalcin A, Weber K, Tuschl T. Duplexes of 21-nucleotide RNAs mediate RNA interference in cultured mammalian cells. Nature 2001; 411:494-8. [PMID: 11373684].

23. Reich SJ, Fosnot J, Kuroki A, Tang W, Yang X, Maguire AM, Bennett J, Tolentino MJ. Small interfering RNA (siRNA) targeting VEGF effectively inhibits ocular neovascularization in a mouse model. Mol Vis 2003; 9:210-6. [PMID: 12789138].

24. Shen J, Samul R, Silva RL, Akiyama H, Liu H, Saishin Y, Hackett SF, Zinnen S, Kossen K, Fosnaugh K, Vargeese C, Gomez A, Bouhana K, Aitchison R, Pavco P, Campochiaro PA. Suppression of ocular neovascularization with siRNA targeting VEGF receptor 1. Gene Ther 2006; 13:225-34. [PMID: 16195704].

25. Miyake K, Miyake N, Yamazaki Y, Shimada T, Hirai Y. Serotype-independent method of recombinant adeno-associated virus (AAV) vector production and purification. J Nippon Med Sch 2012; 79:394-402. [PMID: 23291836].

26. Askou AL, Pournaras JA, Pihlmann M, Svalgaard JD, Arsenijevic Y, Kostic C, Bek T, Dagnaes-Hansen F, Mikkelsen JG, Jensen TG, Corydon TJ. Reduction of choroidal neovascularization in mice by adeno-associated virus-delivered anti-vascular endothelial growth factor short hairpin RNA. J Gene Med 2012; 14:632-41. [PMID: 23080553].

27. Naito Y, Yamada T, Ui-Tei K, Morishita S, Saigo K. siDirect: highly effective, target-specific siRNA design software for mammalian RNA interference. Nucleic Acids Res 2004; 32:W124-9-[PMID: 15215364].

28. Hao DL, Liu CM, Dong WJ, Gong H, Wu XS, Liu DP, Liang CC. Knockdown of human p53 gene expression in 293-T cells by retroviral vector-mediated short hairpin RNA. Acta Biochim Biophys Sin (Shanghai) 2005; 37:779-83. [PMID: 16270158].

29. Ro S, Hwang SJ, Ordög T, Sanders KM. Adenovirus-based short hairpin RNA vectors containing an EGFP marker and mouse U6, human H1, or human U6 promoter. Biotechniques 2005; 38:625-7. [PMID: 15884680].

30. Takahashi H, Kato K, Miyake K, Hirai Y, Yoshino S, Shimada T. Adeno-associated virus vector-mediated anti-angiogenic gene therapy for collagen-induced arthritis in mice. Clin Exp Rheumatol 2005; 23:455-61. [PMID: 16095112].

31. Igarashi T, Miyake K, Asakawa N, Miyake N, Shimada T, Takahashi H. Direct Comparison of Administration Routes for AAV8-mediated Ocular Gene Therapy. Curr Eye Res 2013; 38:569-77. [PMID: 23489150].

32. Singerman L. Combination therapy using the small interfering RNA bevasiranib. Retina 2009; 29:S49-50. [PMID: 19553802].

33. Kaiser PK, Symons RC, Shah SM, Quinlan EJ, Tabandeh H, Do DV, Reisen G, Lockridge JA, Short B, Guerciolini R, Nguyen QD. RNAi-based treatment for neovascular age-related macular degeneration by Sirna-027. Am J Ophthalmol 2010; 150:33-9. [PMID: 20609706].

34. Kleinman ME, Yamada K, Takeda A, Chandrasekaran V, Nozaki M, Baffi JZ, Albuquerque RJ, Yamasaki S, Itaya M, Pan Y, Appukuttan B, Gibbs D, Yang Z, Kariko K, Ambati BK, Wilgus TA, DiPietro LA, Sakurai E, Zhang K, Smith JR, Taylor EW, Ambati J. Sequence- and target-independent angiogenesis suppression by siRNA via TLR3. Nature 2008; 452:591-7. [PMID: 18368052].

35. Ashikari M, Tokoro M, Itaya M, Nozaki M, Ogura Y. Suppression of laser-induced choroidal neovascularization by nontargeted siRNA. Invest Ophthalmol Vis Sci 2010; 51:3820-4. [PMID: 20130283].

36. Gu L, Chen H, Tuo J, Gao X, Chen L. Inhibition of experimental choroidal neovascularization in mice by anti-VEGFA/VEGFR2 or non-specific siRNA. Exp Eye Res 2010; 91:433-9. [PMID: 20599960].

37. Kleinman ME, Kaneko H, Cho WG, Dridi S, Fowler BJ, Blandford AD, Albuquerque RJ, Hirano Y, Terasaki H, Kondo M, Fujita T, Ambati BK, Tarallo V, Gelfand BD, Bogdanovich S, Baffi JZ, Ambati J. Short-interfering RNAs induce retinal degeneration via TLR3 and IRF3. Mol Ther 2012; 20:101-8. [PMID: 21988875].

38. Dinculescu A, Glushakova L, Min SH, Hauswirth WW. Adeno-associated virus-vectored gene therapy for retinal disease. Hum Gene Ther 2005; 16:649-63. [PMID: 15960597].

39. Mussolino C, della Corte M, Rossi S, Viola F, Di Vicino U, Marrocco E, Neglia S, Doria M, Testa F, Giovannoni R, Crasta M, Giunti M, Villani E, Lavitrano M, Bacci ML, Ratiglia R, Simonelli F, Auricchio A, Surace EM. AAV-mediated photoreceptor transduction of the pig cone-enriched retina. Gene Ther 2011; 18:637-45. [PMID: 21412286].

40. Justilien V, Pang JJ, Renganathan K, Zhan X, Crabb JW, Kim SR, Sparrow JR, Hauswirth WW, Lewin AS. SOD2 knockdown mouse model of early AMD. Invest Ophthalmol Vis Sci 2007; 48:4407-20. [PMID: 17898259].

41. Stieger K, Colle MA, Dubreil L, Mendes-Madeira A, Weber M, Le Meur G, Deschamps JY, Provost N, Nivard D, Cherel Y, Moullier P, Rolling F. Subretinal delivery of recombinant AAV serotype 8 vector in dogs results in gene transfer to neurons in the brain. Mol Ther 2008; 16:916-23. [PMID: 18388922].

42. Igarashi T, Miyake K, Kato K, Watanabe A, Ishizaki M, Ohara K, Shimada T. Lentivirus-mediated expression of angiostatin efficiently inhibits neovascularization in a murine proliferative retinopathy model. Gene Ther 2003; 10:219-26. [PMID: 12571629].

Articles are provided courtesy of Emory University and the Zhongshan Ophthalmic Center, Sun Yat-sen University, P.R. China. The print version of this article was created on 11 April 2014. This reflects all typographical corrections and errata to the article through that date. Details of any changes may be found in the online version of the article.